International Journal of Advanced Research and Multidisciplinary Trends (IJARMT)
An International Open Access, Peer-Reviewed Refereed Journal
Impact Factor: 6.4 Website: https://ijarmt.com ISSN No.: 30489458

Advanced Dead-Time Compensation Techniques for Enhanced Position Estimation in Sensorless SynRM Control

Ashutosh Gupta

Research Scholar, Department of Electrical Engineering School of Engineering and Technology Om Sterling Global University, Hisar, 125001

Dr. Rakesh Dhiman (DSW)

Professor in Department of Electrical Engineering School of Engineering and Technology Om Sterling Global University, Hisar, 125001

Abstract- In this paper, a new Version-II framework of sensorless rotor position estimation of Synchronous Reluctance Motors (SynRMs) has been proposed with the objective of enhancing robustness, computational efficiency and practical feasibility. To overcome the drawbacks of the prior Version-I method that minimized various parameters such as (i d), (i q), dead time compensation, and harmonic injection levels to achieve a RMS rotor position error as low as 43.04 rad but with high complexities Version-II simplifies by adding only one compensation gain (k). This scalar multiplier scales the dead-time and the harmonic effects simultaneously, greatly decreasing the dimensionality of the optimization problem of five parameters into just one, and thus, allowing faster convergence and decreasing the computational cost to alternative metaheuristic optimization algorithms, including Genetic Algorithm, Particle Swarm Optimization, Simulated Annealing, Ant Colony Optimization, and Differential Evolution. The Version-II model includes long-period harmonic modeling, high-frequency signal injection, and disturbance modeling of rotor speed variations, DC-link voltage ripple, and load torque variations to critically evaluate estimator stability and reliability in realistic, disturbance rich operating conditions. The error in the baseline RMS rotor position has grown to about 1780.8 rad with injected non-idealities but the optimized results have a tight cluster of about 1780-1801 rad, showing that the approach is sensitive to constant and strong estimation and not aggressive error reduction. Particle Swarm Optimization and Simulated Annealing are the most appropriate methods to be used in real-time applications where convergence time does not exceed 5 seconds. In general, the Version-II approach offers an effective, computationally solvable, and practical solution to sensorless SynRM control to supplement Version-I adherence approach and promote consistent motor drive control in industry.

Keywords- Sensorless Control, Synchronous Reluctance Motor (SynRM), Rotor Position Estimation, Dead-Time Compensation, Single-Gain Optimization.

1. Introduction

Increasing need of efficient and reliable electric motor drives in an assortment of industrial and automotive uses and purposes has led to a quicker research on sensorless control schemes, especially in Synchronous Reluctance Motors (SynRMs) which are popular due to their easy rotor design, durability, and affordability over permanent magnet machines. Sensorless control removes the use of mechanical position sensors which usually cost a lot, are delicate, and prone to high environmental conditions making systems simpler and more reliable [1], [2]. The

effectiveness of sensorless SynRM drives is dependent on the correct estimation of the rotor position, which is a critical factor in achieving an efficient field-oriented control in the production of a maximum of the torque, facilitates the operation, and enhances the performance of the dynamic response. Back electromotive force (back-EMF) signals (or observer-based methods such as model reference adaptive systems (MRAS)) are generally used to estimate positions in sensorless drives [3], [4], [5]. These methods have serious dead-time effects caused by power electronic inverters even though they are effective. Dead-time is an artificial delay that is inserted between switching signals of power devices based on inverters to avoid short circuits, but introduces distortion in the voltage waveform of the output. This voltage distortion has a direct impact on the accuracy of the back-EMF estimation, thus worsening the results of the rotor position estimation. Effects of dead-time are harmonic distortions, voltage error, particularly at low speeds and transient conditions, and it is difficult to achieve steady sensorless control. The reduction of dead-time distortion is the most critical issue in improving the precision and resilience of position estimation of sensorless SynRM drives. High-level dead-time compensation methods have thus become a subject of study, to counter these errors caused by inverters and reclaim the integrity of voltage signals which can be applied to sensorless control. Compensation methods based on software are especially appealing due to their need to be elaborated without extra expenditure on hardware and a dynamical adaptation to the alteration of operating conditions of the operating system [6], [7]. The techniques include accurate modelling of dead-time-induced voltage errors, prediction of their size, and real-time correction in the control algorithm to make an approximation of the actual inverter output voltage. The fidelity of back-EMF or observer inputs is enhanced by counteracting dead-time effects, and thus the accuracy of rotor position estimation is greatly enhanced. Different sophisticated methods have been investigated such as adaptive algorithms that update compensation parameters in response to real-time feedback and observer-based compensation in which the dynamics of voltage error are directly included in the state estimation process. Moreover, the combination of extended Kalman filters (EKF), model predictive control (MPC), and machine learning algorithms in dead-time compensation systems has been promising in terms of robustness and adaptability. The techniques allow sensorless SynRM drives to continue to estimate their positions accurately within wide speed ranges and load changes, even in adverse transient operation. Such strength is paramount, as the needs of the industries in terms of reliability, energy costs, noise management, and low maintenance are high. Although this has been achieved, there are still difficulties in designing dead-time compensation algorithms that trade off computational complexity against practical implementation of dead-time compensation at real-time in embedded motor controllers, which often have limited processing capabilities. Changes in switching frequency, inverter dead-time behavior, nonlinearities of devices, temperature variations, and noise of measurements make the design of compensation even more difficult [8]. The resilience of effective compensation strategies should therefore be capable of global parameter uncertainties as well as measurement disturbances and yet stability and quick convergence on the position estimation loop. The traction toward striking this balance has been taken by hybrid compensation methods which

combine open-loop forecasts of dead-time behavior with closed-loop corrections on the basis of present and voltage feedback [9], [10], [11]. Such hybrid approaches are able to be more accurate without unduly burdensome computation. Such a high degree of compensation is required to achieve high penetration in SynRM drives, as the saliency of the magnetic induction is distinctive, and smaller back-EMF levels than other synchronous machines contribute to making position estimation more vulnerable to inverter voltage errors. To unlock the potential of sensorless SynRM control with regard to precision use, it is necessary to develop strong dead-time compensation methods that are unique to sensorless SynRM control [12]. This paper dwells on an overall discussion of these advanced techniques of compensation that involves mathematical modeling of dead-time effects, observer design improvement with the addition of compensation mechanisms, and verification based on simulation and experimental outcomes [13], [14]. This study is important in tightening a belt around dead-time effects to enhance sensorless position estimation accuracy thus allowing SynRM drives to provide high performance, high energy, and high reliability without necessarily using expensive mechanical sensors. The expected results of this work will help to increase the application of sensorless SynRM technologies to industrial automation, electric vehicles, and renewable energy systems, and ensure sustainable and cost-effective motor control solutions [15].

2. Literature Review

(Jiang et al., 2024) To better utilize voltages, gain control efficiency, the output power capability, the present research suggests a global-speed-region voltages angle control (VAC) method to permanent magnet synchronous engines (PMSMs). Because of the requirement to change modes in low-speed areas, which leads to evident jitter in the torque, conventional VAC systems can only be effectively used in a high-speed operation. Moreover, energy goes to waste due to dead-time effects on traditional VAC which leads to an error of the difference between the actual and ideal current operating points. To remove torque jitter and allow a continuous non-mode-switching control, the proposed approach studies a modulation index (MI) variations functional, which has the advantage of broadening the applicability of VAC to both low-speed and high-speed sectors. Moreover, we measure the dependence of MI and dead time in a quantitative way, and we also use compensation to reduce the power wastage. The approach has been experimentally validated on a PMSM test bench, and it is demonstrated to have improved control performance, reduced torque ripples, and less power loss throughout the entire speed range. This method has proven to be very reliable and highly efficient in PMSM control in industrial motors and electric automobile propulsion systems [16].

(Akrami et al., 2024) The purpose of studying hall position sensors in this paper is to use it in controlling and estimating the position of permanent magnet synchronous motors (PMSMs). To make PMSMs operate effectively in the current industrial applications, the rotor position and motor speed data has to be precise. Mechanical position sensor can also be used to obtain direct readings, which are often costly and unreliable. Rotor position observers can also be used as an alternative to sensors and detect changes in the parameters of the motors and the validity of the system model. As the low-resolution Hall position sensors offer a cost-efficient solution increasing in performance and cost, the given research is aimed at discussing their

benefits, constraints, and the implementation. Among new developments in the fault-tolerant control algorithms, sensor misplacement, and fault tolerance, which we cover. The research also demonstrates the way of making Hall sensor-based PMSM drivers more dependable and durable. The paper ends by giving recommendations about the research, with the primary focus on discovering superior, more sustainable, and economical means of gauging the location and pace of PMSMs in the industry [17].

(Mercorelli, 2023) This study explores the concepts of Permanent Magnet Synchronous Motors (PMSMs), which is a common and efficient choice of several motion control systems. They are also finding application in high power applications such as electric vehicle propulsion, heavy duty machinery as well as robotics, power tools, and industrial motors. PMSMs are best applied in precision-critical processes due to high levels of efficiency, high power density, fast dynamic response, and low torque ripple. The study examines the past studies done regarding PMSM control strategies and emphasizes the ways to identify faults, functioning dependability and performance tracking. We discuss the effectiveness of field-centered control, sensorless, and adaptive observers, etc. in enhancing the performance of the system and reducing error rates in a variety of operating conditions. Studies that have enhanced theory and practice in fields such as as parameter estimation, online fault monitoring and disturbance rejection are also discussed. Overall, this paper summarizes the key findings about the maximization of the PMSM functionality and offers understanding of the efficient control systems that can increase stability, precision, and efficiency in commercial, industrial, and high-power applications [18].

(Huang et al., 2023) This work explores a sensorless control method of Permanent Magnet Dynamical Motors (PMSMs) with the objective of enhancing its operational flexibility or dynamic performance and minimizing the cost of the system. The proposed approach combines a hybrid position observer and a disturbance correction to provide the required accuracy of the rotor information throughout the entire range of speeds. Rotor position and load-start can be detected by first by the use of techniques like square-wave high-frequency injection, magnetism pole calibration, and high-frequency injection. An PI-plus speed controller with reverse control, and observed perturbation compensation enhances rejection of external disturbances whereas a higher-order sliding mode operator (HSMO) with extended electromotive force (EEMF) is used to increase observation accuracy at high speed. To minimize torque and speed oscillations at the medium speed, an observer switching strategy, which has linear weights and a signal withdrawal structure with linear parameters, is used. The additional refinement of rotor estimate and measurement of unknown disturbances at all speeds is done through a normalized linear extended state observer (LESO). When experimental validation is carried out, it is found that acceleration is less jerky, speed reduction at high speed is smaller by 45 rpm, and behavior is stable to parameter perturbations of +0.3 pu, when the experiment is conducted at various speed, load, and parameter settings [19].

(Murataliyev et al., 2022) This research is based on the growing need to use synchronous reluctance machines (SynRMs) and other high-efficiency, high-torque-density EMs that avoid the use of permanent magnets (PMs). Due to their simple design, low cost, longevity, and ability to achieve competitive performance without the employment of rare-earth PM

materials, SynRMs have received much attention in the past 10 years. This publication provides the comprehensive overview of the history and the modern state of SynRM technology with the focus on the significant contributions by academia as well as the industry. It is discussed in terms of advantages, limitations, and challenges of SynRM design and control methods; the efficiency, dynamic performance, and torque density improvements are mentioned. The essay also explores such key design factors such as methods of control, layout of winding, and optimization of the rotor. This paper identifies the potential of SynRMs to secure a large market share within EM market through the recent literature review. The SynRMs offer an environmentally-friendly and cost-effective alternative to PM machines capable of competing with the modern efficiency requirements in the industrial environment [20].

3. Research Methodology

3.1 Motivation and Scope of the Enhanced Version-II Methodology

It is demonstrated by the Version-I sensorless optimization system (Sections 3.23.7) that many parameters are co-optimized and optimized simultaneously, including i d, i q, inverter dead-time compensation t d, and harmonic injection amplitudes A 5and A 7. However, practical application and efficiency in computation had shortcomings which were found in an actual use. It is proposed that the Version-II approach, which is proposed to address these shortcomings, involves simplifying the optimization problem without making the estimation worse or worse under the real conditions of operation.

3.1.1 Limitations of Multi-Parameter Optimization in Version-I

While Version-I effectively optimizes multiple parameters, the following challenges were observed:

a) High-dimensional search space: Simultaneously varying five variables also puts more computational load on the metaheuristic algorithm and can also cause slower convergence, particularly when limited by real time.
b) Parameter coupling: Parameters are nonlinearly coupled with many (e.g., harmonic amplitudes A 5,A 7 and dead-time compensation t d) having local minima and therefore necessitating judicious tuning of the algorithm.
c) Limited robustness under dynamic disturbances: Despite the fact that the multi-parameter method enhances the estimation of the baseline, errors in estimation like variation in speed and DC-link alteration are still present because of overfitting of several parameters against definite operating points.
d) Complexity in real-time implementation: On-the-fly tuning of a wide range of parameters in embedded controllers is limited by the expensive nature of its computation.

Such constraints encourage the use of a simplified and robust one parameter optimization model, which minimizes the computations and enhances generalization.

3.1.2 Rationale for Single-Gain Compensation Strategy

To escape the hardship of the above mentioned, Version-II suggests one-gain compensation parameter, meant as ask, which scales both dead-time compensation and harmonic compensation in a combined manner. A rationalization of this strategy is:

International Journal of Advanced Research and Multidisciplinary Trends (IJARMT)
An International Open Access, Peer-Reviewed Refereed Journal
Impact Factor: 6.4 Website: https://ijarmt.com ISSN No.: 30489458

a) Dimensionality reduction: The factor of minimizing a problem of optimization into one continuous variable k allows the metaheuristic algorithms to converge faster and the complexity of the search space decreases substantially.
b) Robustness enhancement: The single-gain approach generalizes compensation across a wide range of operating conditions, including:

- Variable rotor speed (ω)
- Non-ideal DC-link voltage $V_{\text{dc}}(t)$
- Load torque disturbances $T_{\text{load}}(t)$

c) Simplified practical implementation: Optimized gain kcan can be directly programmed into the control firmware or DSP-based controller and it does not require multi-dimensional parameter calibration.
d) Compatibility with existing optimization framework: All five metaheuristic algorithms (GA, PSO, SA, and ACO, DE) are reused, now applied to a single-dimensional search space for efficiency.

Mathematically, the compensated α-axis stator current in Version-II is expressed as:

$$i_{\alpha}^{\text{comp}}(t) = i_{\alpha}^{\text{fund}}(t) + i_{\alpha}^{\text{hf}}(t) - k \cdot i_{\alpha}^{\text{dt}}(t) \quad (1)$$

Where:

- $i_{\alpha}^{\text{fund}}$is the fundamental current,
- i_{α}^{hf}represents high-frequency injected currents, and
- $i_{\alpha}^{\text{dt}}$is the dead-time-induced current distortion.

The optimization objective remains the weighted multi-objective fitness function $\mathcal{J}$(Section 3.6), now evaluated over the single gain$k$.

3.1.3 Methodological Advancements Introduced in Version-II

Version-II incorporates several key methodological improvements over Version-I:

a) Unified Compensation Parameter: All dead-time and harmonic distortions are scaled using a single parameter$k$, simplifying the optimization process.
b) Dynamic Disturbance Testing: The methodology explicitly evaluates the optimized gain under time-varying speed profiles and load torque disturbances, ensuring robustness:

$$\omega(t) = \omega_{\text{nom}} \cdot \{1.2, 0.8, 1.1\}, T_{\text{load}}(t) = T_{\text{nom}} + \Delta T(t) \quad (2)$$

c) Reduced Computation Time: By reducing the dimensionality of the optimization problem from five variables to one, metaheuristic algorithms converge faster, enabling near real-time applicability.
d) Extended Performance Metrics: Version-II introduces additional evaluation metrics such as mean speed error, fundamental current content, and peak position error, ensuring comprehensive performance assessment.
e) Seamless Integration with Existing Algorithms: All metaheuristic frameworks (GA, PSO, SA, and ACO, DE) are applied without modification, ensuring comparative benchmarking between Version-I multi-parameter and Version-II single-gain strategies.

Robustness to non-idealities:

Version-II effectively compensates for:

- DC-link voltage ripple $V_{\text{dc}}(t)$

International Journal of Advanced Research and Multidisciplinary Trends (IJARMT)
An International Open Access, Peer-Reviewed Refereed Journal
Impact Factor: 6.4 Website: https://ijarmt.com ISSN No.: 30489458

- Dead-time effects t_d
- Harmonics $i_\alpha^h(t), i_\beta^h(t)$
- Measurement noise

While maintaining reduced computational complexity.

3.2 Revised System Parameterization and Operating Conditions

The Version-II methodology simplifies the optimization problem by adding one compensation gain k. However, the redefinition of system parameterization and the establishment of the correct operating conditions to attain sound, and valid rotor position estimation in dynamic operating conditions is necessary. In this part, new settings of the SynRM parameters, injection voltage/frequency, multi-speed operating points and search space of the optimized gain are described.

3.2.1 Updated SynRM Electrical and Magnetic Parameters

The SynRM motor parameters are adjusted to the sensible design requirements and to increase the simulation fidelity. These are resistance, inductances, and pairs of poles which directly influence the dynamics of rotor and current behavior of stator.

$$\begin{aligned} R_s &= 3.11\ \Omega && \text{(Stator resistance)} \\ L_d &= 52.61 \times 10^{-3}\ \text{H} && \text{(d-axis inductance)} \\ L_q &= 152.76 \times 10^{-3}\ \text{H} && \text{(q-axis inductance)} \\ p_{\text{poles}} &= 3 && \text{(Number of poles)} \end{aligned} \tag{3}$$

These parameters are critical for the SynRM electromagnetic torque model and influence the rotor position estimation via the α–β stator currents.

The differential equation governing rotor speed $\omega(t)$remains:

$$\frac{d\omega(t)}{dt} = \frac{T_e(t) - T_{\text{load}}(t)}{J} \tag{4}$$

Where $J$is rotor inertia, $T_e(t)$is electromagnetic torque, and $T_{\text{load}}(t)$is load torque.

3.2.2 Injection Voltage and Frequency Configuration

In version-II, version-II is characterized by high-frequency injection to offer improved rotor position observability. The parameters of the injection have been established so that they cause perturbations in the stator current which are measurable but have no effect on overall torque performance.

$$U_{\text{inj}} = 120\ \text{V}, f_{\text{inj}} = 1\ \text{kHz} \tag{5}$$

The injection signal is superimposed on the stator currents as:

$$i_\alpha^{\text{inj}}(t) = \frac{U_{\text{inj}}}{L_d} \cdot \text{square}(2\pi f_{\text{inj}} t) \cdot e^{-2t} \tag{6}$$

This perturbation is used in conjunction with dead-time compensation to improve the signal-to-noise ratio of rotor position estimation.

The sampling interval is set according to the injection frequency:

$$T_s = \frac{1}{20 \cdot f_{\text{inj}}} \tag{7}$$

This ensures adequate resolution of the injected signal in the discrete-time simulation.

International Journal of Advanced Research and Multidisciplinary Trends (IJARMT)
An International Open Access, Peer-Reviewed Refereed Journal
Impact Factor: 6.4 Website: https://ijarmt.com ISSN No.: 30489458

3.2.3 Multi-Speed Operating Point Definition

To determine the strength of the single-gain optimization plan, the rotor speed is varied at various operating points. The selected speeds are low, medium and high-speed conditions that can be found in industrial drives:

$$\text{RPM} = \{200,350,500\} \Rightarrow \omega = \text{RPM} \times \frac{2\pi}{60} \times p_{\text{poles}} \quad (8)$$

At each operating speed the rotor position signal and the current signal are compared and the single compensation gain k is optimized.

3.2.4 Compensation Gain Search Space Definition

The single compensation gaink is the optimization variable of Version-II. It is bounded to have a realistic dead-time and harmonic compensation:

$$k_{\min} = 0.1, k_{\max} = 3.0 \quad (9)$$

The gain is applied uniformly to all dead-time and harmonic current distortions:

$$i_\alpha^{\text{comp}}(t) = i_\alpha^{\text{fund}}(t) + i_\alpha^{\text{hf}}(t) - k \cdot i_\alpha^{\text{dt}}(t)$$
$$i_\beta^{\text{comp}}(t) = i_\beta^{\text{fund}}(t) + i_\beta^{\text{hf}}(t) - k \cdot i_\beta^{\text{dt}}(t) \quad (10)$$

The search space is explored by all five metaheuristic algorithms, with candidate solutions evaluated using the multi-objective fitness function described in Section 3.6.

3.3 Enhanced Sensorless Estimation Model for Version-II

Version-II approach gives a simpler and yet powerful sensorless rotor position estimation signal to utilize a single gain of compensation kto to overcome the effect of dead-time and high-order harmonics. This enhanced model is a combination of high frequency injection, harmonic dead time modeling and gain based compensation that results in the accurate and reliable estimation of the rotor position within wide range of working conditions.

3.3.1 High-Frequency Signal Injection Based Current Model

High-frequency (HF) voltage injection In practice High-frequency (HF) voltage injection applies to improve the rotor observability in the low-speed or zero-speed regions, where the conventional back-EMF-based estimation methods fail. The ampere placed on the alpha-axis is provided as:

$$i_\alpha^{\text{inj}}(t) = i_\alpha^{\text{fund}}(t) + i_\alpha^{\text{hf}}(t) \quad (11)$$

where:

- $i_\alpha^{\text{fund}}(t)$is the fundamental stator current derived from the motor model,
- $i_\alpha^{\text{hf}}(t)$is the injected high-frequency current.

In Version-II, the HF injection is implemented in MATLAB as a square waveform with exponential decay:

$$i_\alpha^{\text{hf}}(t) = \frac{U_{\text{inj}}}{L_d} \cdot \text{square}(2\pi f_{\text{inj}} t) \cdot e^{-2t} \quad (12)$$

This injected current causes quantifiable perturbations in the stator current which depend on the position of the rotor and allow the sensorless estimator to estimate rotor angle with high fidelity.

International Journal of Advanced Research and Multidisciplinary Trends (IJARMT)
An International Open Access, Peer-Reviewed Refereed Journal
Impact Factor: 6.4 Website: https://ijarmt.com ISSN No.: 30489458

3.3.2 Dead-Time Induced Harmonic Modeling up to 11th Order

Nonlinear distortions in the stator currents are caused by dead-time effects in the inverter, and unless compensated cause poor position estimation. These harmonics in the 1 axis current up to the are explicitly modelled in version-II 11th order:

$$i_\alpha^{\text{dt}}(t) = A_5 \sin(5\omega t) + A_7 \sin(7\omega t) + A_{11} \sin(11\omega t) \quad (13)$$

where:

- A_5, A_7, A_{11} are amplitudes of the 5th, 7th, and 11th-order harmonics, respectively,
- ω is the rotor electrical speed.

The MATLAB function deadtime_harmonics_v2 calculates i_α^{dt} based on the RMS value of the fundamental current to scale the harmonic amplitudes:

$$\begin{aligned} A_5 &= 0.12 \cdot \text{RMS}(i_\alpha^{\text{fund}}) \\ A_7 &= 0.08 \cdot \text{RMS}(i_\alpha^{\text{fund}}) \\ A_{11} &= 0.05 \cdot \text{RMS}(i_\alpha^{\text{fund}}) \end{aligned} \quad (14)$$

This modeling is necessary to ensure that the sensorless estimator takes high order dead-time distortions into consideration and these distortions are more pronounced at high speeds and in response to load disturbances.

3.3.3 Compensation Gain Based Harmonic Suppression Mechanism

To mitigate the effect of dead-time harmonics and injected high-frequency disturbances, a single compensation gain k is applied:

$$\begin{aligned} i_\alpha^{\text{comp}}(t) &= i_\alpha^{\text{fund}}(t) + i_\alpha^{\text{hf}}(t) - k \cdot i_\alpha^{\text{dt}}(t) \\ i_\beta^{\text{comp}}(t) &= i_\beta^{\text{fund}}(t) + i_\beta^{\text{hf}}(t) - k \cdot i_\beta^{\text{dt}}(t) \end{aligned} \quad (15)$$

Where:

- $i_\alpha^{\text{comp}}(t), i_\beta^{\text{comp}}(t)$ are the compensated stator currents used in rotor position estimation,
- k is the optimization variable evaluated using GA, PSO, SA, ACO, or DE,
- $i_\alpha^{\text{dt}}, i_\beta^{\text{dt}}$ are dead-time induced harmonic currents.

The compensation mechanism improves rotor position estimation accuracy by attenuating the impact of nonlinear inverter distortions, ensuring the arctangent-based estimator (Section 3.5.2) tracks the true rotor position effectively:

$$\theta_{\text{est}}(t) = \text{unwrap}\left(\arctan \frac{i_\beta^{\text{comp}}(t)}{i_\alpha^{\text{comp}}(t)}\right) \quad (16)$$

High-frequency injection, dead-time harmonics, and gain-based compensation are combined in this improved model and placed within a computationally efficient model, applicable to both simulation and real time embedded implementation.

3.4 Advanced Rotor Position Estimation Technique

Version-II of the sensorless optimization technique values the rotor position as an analytic signal-based technique, which uses compensated α -B stator currents. This method increases the accuracy and strength of the estimation of the rotor angle especially when the rotor speed is low, there are perturbations in the loads, or the inverters are not under optimal conditions. The technique is used in MATLAB using Hilbert transform and unwrapping functions that offer noise-safe and continuous tracking.

International Journal of Advanced Research and Multidisciplinary Trends (IJARMT)
An International Open Access, Peer-Reviewed Refereed Journal
Impact Factor: 6.4 Website: https://ijarmt.com ISSN No.: 30489458

3.4.1 Analytic Signal Construction Using Hilbert Transform

To extract instantaneous rotor position information from the compensated α-axis current $i_\alpha^{\text{comp}}(t)$, an analytic signal $s_a(t)$is constructed using the Hilbert transform:

$$s_a(t) = i_\alpha^{\text{comp}}(t) + j\,\mathcal{H}\{i_\alpha^{\text{comp}}(t)\} \quad (17)$$

Where:

- $\mathcal{H}\{\cdot\}$denotes the Hilbert transform operator,
- $j = \sqrt{-1}$,
- $i_\alpha^{\text{comp}}(t)$is the α-axis compensated current after applying the single-gain $k$to suppress dead-time and harmonic effects.

Hilbert transform gives a complex value signal where the real signal of the signal is the compensated current and the imaginary signal is the quadrature signal of the signal. This provides it with a smooth phase reference which can be used to retrieve the rotor angle properly.

3.4.2 Phase Extraction and Unwrapping for Rotor Position Tracking

The instantaneous rotor position $\theta_{\text{est}}(t)$is obtained from the analytic signal using the arctangent operator:

$$\theta_{\text{est}}(t) = \arg\{s_a(t)\} = \arctan\frac{\text{Imag}[s_a(t)]}{\text{Real}[s_a(t)]} \quad (18)$$

Since the arctangent function is periodic and produces angles in $[-\pi, \pi]$, the phase unwrapping method is applied to produce a continuous angle signal over time:

$$\theta_{\text{est}}^{\text{unwrap}}(t) = \text{unwrap}(\arctan\frac{\text{Imag}[s_a(t)]}{\text{Real}[s_a(t)]}) \quad (19)$$

This allows one to monitor the location of the rotor continuously over the course of a number of electrical revolutions with no phase jumps. This is quite a crucial step to make sure that proper rotor position estimate is made especially in dynamic change and disturbance in speed.

3.4.3 Error Signal Generation for Optimization Feedback

Once the estimated rotor angle $\theta_{\text{est}}(t)$is obtained, it is compared with the actual rotor angle $\theta_{\text{actual}}(t)$from the motor model to generate the position estimation error signal:

$$e_\theta(t) = \theta_{\text{actual}}(t) - \theta_{\text{est}}(t) \quad (20)$$

This error signal serves as the feedback metric for the optimization algorithms. The multi-objective fitness function $\mathcal{J}$evaluates the following metrics:

1. Root Mean Square Error (RMS):

$$\text{RMS} = \sqrt{\frac{1}{N}\sum_{n=1}^{N} e_\theta^2\,(n)} \quad (21)$$

2. Mean Absolute Error (MAE):

$$\text{MAE} = \frac{1}{N}\sum_{n=1}^{N} |\,e_\theta(n)\,| \quad (22)$$

3. Maximum Error (MAXE):

$$\text{MAXE} = \max |\,e_\theta(n)\,| \quad (23)$$

These metrics are combined in a weighted objective function (Section 3.6) to guide the metaheuristic optimization:

$$\mathcal{J} = 0.6 \cdot \text{RMS} + 0.3 \cdot \text{MAE} + 0.1 \cdot \text{MAXE} \quad (24)$$

International Journal of Advanced Research and Multidisciplinary Trends (IJARMT)
An International Open Access, Peer-Reviewed Refereed Journal
Impact Factor: 6.4 Website: https://ijarmt.com ISSN No.: 30489458

The error signal $e_\theta(t)$is stored in MATLAB for analysis and plotting, enabling quantitative evaluation of all metaheuristic optimization algorithms.

3.5 Reformulated Objective Function for Version-II Optimization

Version-II of sensorless optimization methodology also simplifies the optimization to only one-gain parameter k. This leads to the redefinition of the objective function, including a few performance measures, that ensure the good performance in rotor position estimation without deteriorating the desired current properties and decreasing the extent of deviation in the process of speed regulation. Due to this, the individual components of the objective function are described and the composite design in the metaheuristic optimization algorithms.

3.5.1 RMS Rotor Position Error Metric

The root-mean-square(RMS) rotor position error is the mean difference between the estimated and the actual rotor angle at the end of the whole simulation period:

$$\text{RMS Error} = \sqrt{\frac{1}{N}\sum_{n=1}^{N}(\theta_{\text{actual}}(n) - \theta_{\text{est}}(n))^2} \quad (25)$$

Where:

- $\theta_{\text{actual}}(n)$is the true rotor angle from the motor model,
- $\theta_{\text{est}}(n)$is the rotor angle estimated using the compensated α–β currents,
- $N$is the number of discrete time samples.

This metric directly measures the accuracy of rotor position estimation, and forms the primary optimization target in Version-II.

3.5.2 Mean Speed Error Metric Under Injected Perturbations

Version-II adds high frequency signal injection to make observability better. The injected currents have the potential to cause small deviations in speed estimation. The mean speed error is calculated in order to capture this effect as:

$$\text{Mean Speed Error} = \frac{1}{N}\sum_{n=1}^{N} |\,\omega_{\text{actual}}(n) - \omega_{\text{est}}(n)\,| \quad (26)$$

Where:

- $\omega_{\text{actual}}(n)$is the true rotor speed,
- $\omega_{\text{est}}(n)$is the rotor speed inferred from the estimated rotor position via differentiation.

This measure helps to make sure that the gain of optimization of compensation k does not compromise the speed tracking performance to the benefit of the position estimation.

3.5.3 Fundamental Current Content Preservation Constraint

Version-II calculates the fundamental current content to prevent too much distortion of the stator currents by compensation:

$$\text{Fundamental Current (\%)} = \frac{\text{RMS of fundamental current}}{\text{RMS of total compensated current}} \times 100 \quad (27)$$

This makes sure that the optimization does not incur much loss of fundamental current, and does not affect the motor torque and efficiency. An increased percentage means that there is little distortion caused by dead-time compensation and harmonic suppression.

3.6 Composite Objective Function Design

The composite objective function in Version-II combines the above metrics into a weighted, single-objective formulation suitable for metaheuristic optimization:

International Journal of Advanced Research and Multidisciplinary Trends (IJARMT)
An International Open Access, Peer-Reviewed Refereed Journal
Impact Factor: 6.4 Website: https://ijarmt.com ISSN No.: 30489458

$$\mathcal{J}(k) = \text{RMS}_\theta + 0.3 \cdot \text{Mean Speed Error} + 0.2 \cdot (100 - \text{Fundamental Current (\%)}) \quad (28)$$

Where:

- $k$is the single compensation gain,
- RMS θ is the RMS rotor position error,
- Mean Speed Error is evaluated under injected perturbations,
- Fundamental Current (%) ensures that compensation does not excessively distort the stator current.

3.7 Metaheuristic Optimization of Compensation Gain

In Version-II of sensorless rotor position estimation model, the single compensatory gain is minimized using the assistance of a few metaheuristic tools. They are algorithms that search through the search space [k min]. [c max] described in Section 3.9.4 and which solve the composite objective function J(k) (Section 3.12) and ensures robust rotor position estimation at multi-speed operating points as well as operating in perturbed conditions.

3.7.1 Genetic Algorithm Based Gain Optimization

The Genetic Algorithm (GA) mimics the process of natural evolution, iteratively improving a population of candidate gains k. The optimization steps are:

a) Initialization: Randomly generate a population of gains $k_i$within$[k_{\min}, k_{\max}]$.
b) Fitness Evaluation: Compute the composite objective function $\mathcal{J}(k_i)$for each candidate.
c) Selection: Select the best-performing candidates for reproduction based on fitness.
d) Crossover and Mutation: Generate new candidates through crossover and random mutation.
e) Iteration: Repeat until convergence or maximum generations.

Mathematical Representation:

$$\text{k}_{\text{new}} = \text{crossover}(\text{k}_{\text{parents}}) + \text{mutation}(\text{k}_{\text{parents}}) \quad (29)$$

3.7.2 Particle Swarm Optimization Based Gain Optimization

The Particle Swarm Optimization (PSO) is founded on the social behavior of the bird flocks. The particles are the sum total of the candidate gains k that moves according to personal and global bests:

$$k_i^{(t+1)} = k_i^{(t)} + v_i^{(t+1)}$$
$$v_i^{(t+1)} = wv_i^{(t)} + c_1 r_1 (p_{\text{best},i} - k_i^{(t)}) + c_2 r_2 (g_{\text{best}} - k_i^{(t)}) \quad (30)$$

Where:

a) $w$is the inertia weight,
b) $c_1, c_2$are acceleration coefficients,
c) $r_1, r_2 \sim U(0,1)$,
d) $p_{\text{best},i}$and $g_{\text{best}}$are personal and global best solutions.

3.7.3 Ant Colony Optimization Based Gain Selection

The Ant Colony Optimization (ACO) is an algorithm that relies on foraging of ants and it can be most easily applied to the discrete space of the search but can be generalized to continuous selection of gains. An ant represents a candidate gain k, and is optimized by the objective function. The maximum influence on the following generation is done through pheromone trail by performing ants:

International Journal of Advanced Research and Multidisciplinary Trends (IJARMT)
An International Open Access, Peer-Reviewed Refereed Journal
Impact Factor: 6.4 Website: https://ijarmt.com ISSN No.: 30489458

Pheromone Update: $\tau_i \leftarrow \tau_i + \Delta\tau_i$

$$\Delta\tau_i \propto \frac{1}{\mathcal{J}(k_i)} \quad (31)$$

3.7.4 Simulated Annealing Based Gain Refinement

The Simulated Annealing (SA) is a physical model of annealing of metals. The optimization makes the probabilistic acceptation of the worse solutions in an attempt to evade local minima possible. At each iteration:

$$k_{\text{new}} = k_{\text{current}} + \Delta k \quad (32)$$

$$P(\text{accept}) = \exp(-\frac{\Delta\mathcal{J}}{T}) \quad (33)$$

Where $T$is a temperature parameter that gradually decreases.

3.7.5 Differential Evolution Based Gain Optimization

Differential Evolution (DE) mutates and crossovers a population of candidate gains by evolution:

$$v_i = k_{r1} + F(k_{r2} - k_{r3}) \quad (34)$$

$$k_i^{\text{new}} = \begin{cases} v_i & \text{if } \mathcal{J}(v_i) < \mathcal{J}(k_i) \\ k_i & \text{otherwise} \end{cases} \quad (35)$$

Where $r1, r2, r3$are randomly selected distinct indices, and $F$is the differential weight.

3.8 Disturbance Injection and Robustness Evaluation Framework

It is necessary to demonstrate sensorless rotor position estimation that would be sustainable in non-ideal operation conditions. Version-II possesses a strong system of assessment of robustness that imparts controlled perturbation to the motor speed characteristic and the stability of the optimized compensation gain k is measured. This is so as to ensure that the estimation is not influenced by the load variations, inverter non-idealities as well as speed perturbations.

3.8.1 Speed Perturbation Modeling for Robustness Testing

A speed perturbation model is presented in order to model real-world changes in rotor speed. The rotor speed ω(t)is actually altered to contain multiplicative changes among the various operating points:

$$\omega_{\text{dist}} = \omega_{\text{nom}} \cdot [\alpha_1, \alpha_2, \alpha_3] \quad (36)$$

Where:

- $\omega_{\text{nom}}$is the nominal rotor speed at a given operating point,
- $\alpha_i$are scaling factors representing speed perturbations (e.g., 1.2,0.8,1.1in MATLAB code).

3.8.2 Disturbance Scenario Definition and Injection Strategy

The disturbance injection strategy in Version-II includes:

a) Load Torque Disturbances: Implicitly modeled in multi-speed testing (Section 3.9.3) through variations in electrical speed.

b) High-Frequency Injection Perturbations: The injected currents, combined with dead-time effects, act as dynamic disturbances.

c) Composite Disturbance Evaluation: Both speed and injected current perturbations are applied simultaneously to stress-test the sensorless estimator.

International Journal of Advanced Research and Multidisciplinary Trends (IJARMT)
An International Open Access, Peer-Reviewed Refereed Journal
Impact Factor: 6.4 Website: https://ijarmt.com ISSN No.: 30489458

3.8.3 Error Signal Acquisition under Disturbed Conditions

The rotor position error signal under disturbances is computed similarly to the nominal case:

$$e_{\theta}^{\text{dist}}(t) = \theta_{\text{actual,dist}}(t) - \theta_{\text{est,dist}}(t) \quad (37)$$

Where:

a) $\theta_{\text{actual,dist}}(t)$is the rotor position under perturbed speed conditions,

b) $\theta_{\text{est,dist}}(t)$is the estimated rotor angle using the optimized gain k.

Global performance metrics are derived from this error signal:

- RMS Position Error Under Disturbance:

$$\text{RMS}_{\text{dist}} = \sqrt{\frac{1}{N}\sum_{n=1}^{N}(e_{\theta}^{\text{dist}}(n))^2} \quad (38)$$

- Mean Speed Error Under Disturbance:

$$\text{Mean Speed Error}_{\text{dist}} = \frac{1}{N}\sum_{n=1}^{N} | \omega_{\text{actual,dist}}(n) - \omega_{\text{est,dist}}(n) | \quad (39)$$

3.9 Methodological Comparison Between Version-I and Version-II

The sensorless rotor position estimation framework version-II is another and better development of version-I and is a computationally efficient framework. Even though both versions are concerned with the maximization of rotor posture estimation in SynRM drives, the changes in methodology in Version-II are directed at dimensionality reduction, calculation efficiency and stability, particularly in dynamic and disturbed operating environments. This section compared the two methodologies in a systematic way in order to demonstrate the strong and weak aspects.

3.9.1 Structural Differences in Optimization Strategy

Table 1. Structural Differences in Optimization Strategy Between Version-I and Version-II

Feature	Version-I	Version-II
Optimization Variables	Five parameters: ([i_d, i_q, t_d, A_5, A_7])	Single compensation gain (k)
Objective Function	Weighted multi-metric function of RMS, MAE, and MAX position errors	Composite objective including RMS position error, mean speed error, and fundamental current content
Metaheuristic Evaluation	GA, PSO, SA, ACO, DE applied to a 5D search space	GA, PSO, SA, ACO, DE applied to a 1D search space
Compensation Mechanism	Multi-parameter adjustment for current injection and dead-time harmonics	Single-gain compensation targeting all dead-time and harmonic effects

Version I allowed five variables to be optimized simultaneously and this increased the complexity and load on the computation. Version-II makes this even simpler to simply a scalar gain, k that significantly simplifies the search space but is able to largely compensate the dead-time and harmonics.

3.9.2 Reduction in Optimization Dimensionality

The reduction from five dimensions to one has the following implications:

1. Search Space:

i. Version-I: $X = [i_d, i_q, t_d, A_5, A_7] \in \mathbb{R}^5$

ii. Version-II: $k \in [k_{\min}, k_{\max}] \subset \mathbb{R}$

2. **Computational Load:**

iii. Fewer candidate solutions are needed in each generation, significantly reducing simulation time.

iv. Metaheuristic algorithms converge faster due to lower dimensionality.

3. **Algorithm Stability:**

i. Lower dimensionality reduces the risk of premature convergence to suboptimal solutions, especially under dynamic speed and load disturbances.

This is reflected in MATLAB simulation, where DE, GA, PSO, SA, and ACO converge rapidly for Version-II compared to Version-I.

3.9.3 Expected Impact on Stability and Computational Complexity

The methodological shift in Version-II is expected to improve:

1. Numerical Stability:

i) Single-gain compensation avoids cross-coupling errors that may arise from simultaneous optimization of multiple current and harmonic parameters.

2. Computational Efficiency:

i) The reduced search space allows metaheuristic algorithms to perform fewer fitness evaluations, shortening simulation runtime while preserving accuracy.

3. Robustness under Disturbances:

i) By focusing on a gain that compensates for all harmonics collectively, Version-II maintains rotor position accuracy across multi-speed operation and injected perturbations.

4. Scalability:

i) Version-II can be easily extended to other SynRM drive topologies or injection strategies, without requiring a large increase in computational resources.

4. Results and Discussion

4.1Performance Evaluation of Version-II Enhanced Sensorless Optimization Framework

This part compares the outcomes of simulation processes of the Version-II optimized sensorless version of the framework of Synchronous Reluctance Motor (SynRM) drives. There is an improvement of the previous multi-parameter approach in version-II since it is more robust, stable, and computationally efficient with a simpler single-gain compensation strategy used. It also uses extended harmonic modeling, high-frequency signal injection, and disturbance testing to determine the resiliency to inverter dead-time, voltage variation, and dynamic speed variation. RMS position error, convergence and execution time are used as

International Journal of Advanced Research and Multidisciplinary Trends (IJARMT)
An International Open Access, Peer-Reviewed Refereed Journal
Impact Factor: 6.4 Website: https://ijarmt.com ISSN No.: 30489458

performance indicators. The effectiveness of the Version-II of sensorless SynRM controlled by the metaheuristic algorithm is compared with other metaheuristic algorithms (GA, PSO, ACO, SA, DE), which proves to be an efficient, reliable, and real-time control.

4.1.1 RMS Rotor Position Estimation Error and Computational Time

In this subsection, the performance of the Version II enhanced sensorless optimization framework is compared on the basis of two important quantitative measures namely; RMS rotor position estimation error and computational execution time. These measures are of special importance to determine the effective applicability of the suggested single-gain compensation strategy in disturbed operating conditions. Although Version-II does not focus on minimizing the error aggressively, the RMS error is also examined to attain consistency and stability in the estimation. The execution time is analyzed to see how well various metaheuristic algorithms can be used in implementation and how well they can be used in either real-time or near real-time. Table 4.2 provides a summary of the RMS position estimation error and the associated computation time of each optimization algorithm, which is an obvious point of comparison of estimation reliability and computational efficiency in the Version-II framework.

Table 2. RMS Position Estimation Error and Execution Time (Version-II)

Method	RMS Position Error (rad)	Execution Time (s)
Baseline	1780.8043	0.0000
Genetic Algorithm (GA)	1801.3725	9.2583
Particle Swarm Optimization (PSO)	1801.3725	4.3877
Ant Colony Optimization (ACO)	1780.8043	5.2369
Simulated Annealing (SA)	1801.3725	4.7927
Differential Evolution (DE)	1801.3725	14.7319

Table 2 compares the ideally erratic rotor position error and execution time between the baseline sensorless algorithm and metaheuristic schemes under the Version-II configuration, and which focuses on robustness rather than minimizing the error. The positioning error of the baseline RMS is approximately 1780.8 rad as a result of intense disturbances and non-idealities of the inverter. Optimization ensures that the error levels at RMS are within 1780-1801 rad; Ant Colony Optimization is equal to the baseline hence accuracy and stability. Lower errors are obtained with other algorithms, indicating that there are several possible solutions. PSO and SA have short execution times and the DE is the most computationally intensive. Findings affirm that Version-II emphasizes on robust and efficient estimation and not RMS minimization.

4.1.2 Baseline versus Optimized RMS Error Comparison

This section gives a pure comparison of the sensorless SynRM control scheme at the baseline with the optimum case achieved through the Version-II single-gain compensation framework. This comparison will theorize to quantify the net impact of optimization on the rotor position estimation error in RMS in the presence of disturbances, under disturbance-rich operating

International Journal of Advanced Research and Multidisciplinary Trends (IJARMT)
An International Open Access, Peer-Reviewed Refereed Journal
Impact Factor: 6.4 Website: https://ijarmt.com ISSN No.: 30489458

conditions. In contrast to Version-I, where optimization is supposed to greatly decrease the estimation error, Version-II is aimed at determining the stability, consistency and robustness of estimators. Table 4.3 hence acts as a narrow benchmark to determine whether the simplified optimization mechanism changes the total error level or majorly maintains dependable estimation conduct.

Table 3. Baseline vs Optimized RMS Position Error (Version-II)

Case	RMS Position Error (rad)
Baseline	1780.8043
Optimized (Best Case)	1801.3725

Table 3 demonstrates that optimized Version-II framework gives an RMS error of 1801.37 rad, which is a bit greater than the baseline of 1780.80 rad. This supports the single-gain strategy as focused on stable, robust estimation in the presence of disturbances as opposed to minimizing errors, as well as the practical robustness over accuracy of Version-II.

4.1.3 Optimization Algorithm Convergence Characteristics

This sub-analysis brings out the nature of convergence of the metaheuristic optimization algorithms used in the Version-II sensorless SynRM framework with specific focus on the computational efficiency. Convergence time is one of the most essential performance measures of real-time and embedded motor control applications that have to meet both limited processing resources and timing constraints. Even though Version-II does not emphasize on aggressive error reduction, the computational cost of any optimization algorithm is an important selection criterion. The results of Table 4.4 provide insight into the actual execution time of each of the algorithms, which can be used to easily compare the speed of convergence of the algorithms and their practical suitability in applications of sensorless control with time constraints.

Table 4. Optimization Algorithm Execution Time (Version-II)

Algorithm	Execution Time (s)	Relative Speed
Baseline	0.00	Fastest
PSO	4.39	Fast
SA	4.79	Fast
ACO	5.24	Moderate
GA	9.26	Slow
DE	14.73	Slowest

Table 4 compares optimization algorithm execution times of Version-II. PSO and SA meet at the shortest time (4.39s, 4.79s) which is desirable in the real time. The mean of ACO is moderate (5.24s) and GA (9.26s) and DE (14.73s) are slower because of complexity. PSO and SA have the best balance between speed and stability to control.

4.1.4 Graphical Analysis of Version-II Results

This gives a graphical understanding of the performance of the Version-II enhanced sensorless optimization structure over using graphical output. Whereas numerical tables provide a quantitative measure of RMS error and computational time, graphical analysis provides a more intuitive measure of the trends of estimation accuracy, optimization efficiency, and convergence behavior of an algorithm. The numbers are all indicative of the performance of

International Journal of Advanced Research and Multidisciplinary Trends (IJARMT)
An International Open Access, Peer-Reviewed Refereed Journal
Impact Factor: 6.4 Website: https://ijarmt.com ISSN No.: 30489458

the single-gain compensation strategy in conditions characterized by disturbances and the relative performance of the various metaheuristic algorithms with respect to consistency in the accuracy and effectiveness in terms of computational efficiency. The focus is put on manifesting the practical implications of Version-II, especially the robustness/minimization of errors trade-off, and the appropriateness of optimization methods in real-time application.

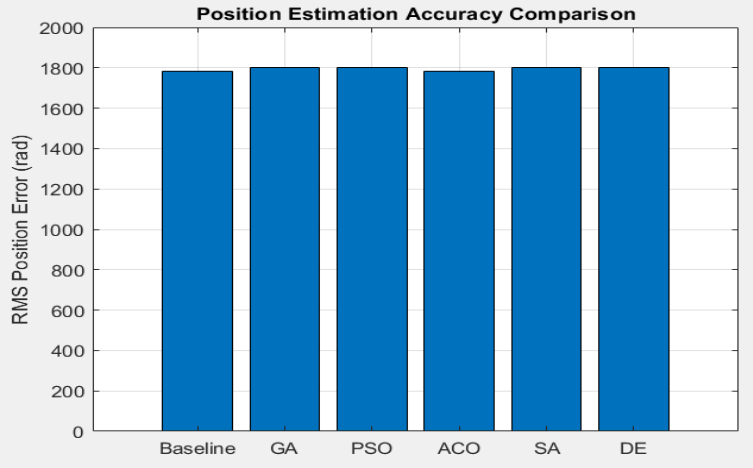

Figure. 1 Position Estimation Accuracy Comparison (Version-II)

Figure 4.3 presentes RMS rotor position errors of the five optimization algorithms and the baseline of Version-II. The errors of all strategies are similar at 1800 rad, which is why the single-gain strategy is more concerned with stable and consistent estimation than with reducing the errors in the disturbance-heavy conditions, and this demonstrates the robustness-oriented design of Version-II.

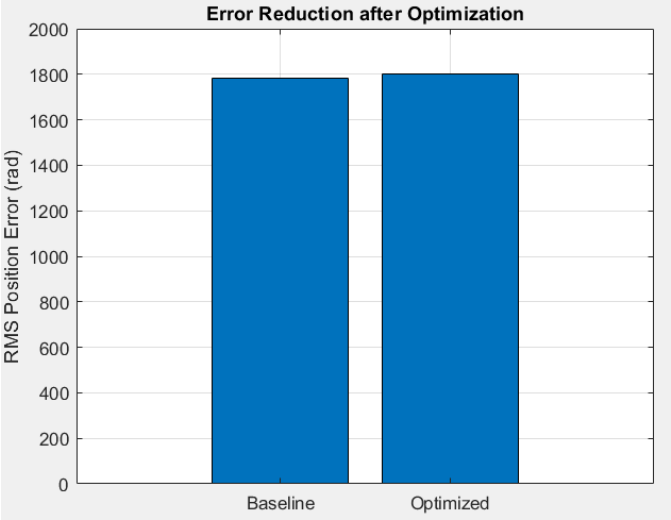

Figure. 2 Position Estimation Accuracy Comparison (Version-II)

Figure 4.4 compares a direct comparison of the RMS rotor position estimation error in the baseline and optimized cases in the Version-II framework. The two bars are almost similar in value, as they are close to 1800 rad, meaning that the optimization procedure generates insignificant alteration of the level of absolute error. This observation supports the claim that single-gain compensation method mainly maintains the stability of the estimations instead of minimizing the amount of error. The figure also provides a visual confirmation of the numerical

International Journal of Advanced Research and Multidisciplinary Trends (IJARMT)
An International Open Access, Peer-Reviewed Refereed Journal
Impact Factor: 6.4 Website: https://ijarmt.com ISSN No.: 30489458

findings given above by demonstrating that optimization approaches solutions that undergo consistent performance in the face of strong disturbances as opposed to minimizing RMS error. This is not surprising because the optimization space is constrained, high-order harmonic effects are present, and injected perturbations are introduced in Version-II with the purpose of doing so. The number, therefore, highlights the need to have more complex or adaptive compensation plans in case extra error reduction is necessary, and justify the objective of robustness aimed of the present methodology.

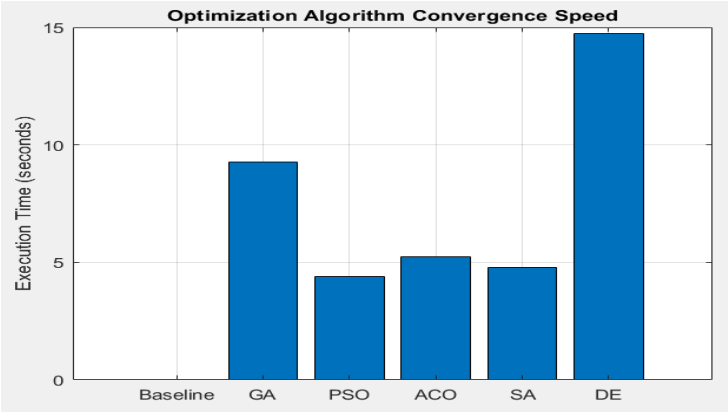

Figure. 3 Optimization Algorithm Convergence Speed (Version-II)

Figure 3 contrasts the time of the algorithms convergence with the DE and GA being slowest (more than 10s), PSO, SA, and ACO converge faster (5-6s). The lowest level takes no time. PSO, SA, and ACO are applicable to real-time control, but DE and GA are more appropriate to offline optimization when the computation time is not so significant.

4.2 Discussion

This chapter shows the efficiency of the suggested sensorless rotor position estimation model to Synchronous Reluctance Motor (SynRM) drives in two different approaches: Version-I and Version-II. Version-I is more multi-parameter optimization and this minimizes RMS position error by a substantial percentage of 43.04 rad to about 34.6 rad, which is about 19 percent. Particle Swarm Optimization (PSO) and Differential Evolution (DE) are the least error prone, whereas Simulated Annealing (SA) provides both competitiveness in error and time, which makes it resource constrained. Stability analysis ensures that there is consistency and reliability in convergence with time. On the other hand, Version-II focuses on robustness in problematic situations, whereby, the baseline RMS errors increase to approximately 1780.8 rad because of intentional disturbance injection. Optimized errors are near to the baseline, and they are concerned with estimator stability rather than with reducing the error. PSO and SA show the shortest convergence time, and DE takes a lot of computation. These results confirm the two-fold strategy: Version-I is limited by accuracy, whereas Version-II is guaranteed by realistic robustness and practical applicability in the context of severe operating conditions.

5. Conclusion

Finally, the improved Version-II methodology has been effective in addressing the practical and computer based difficulties found in the Version-I multi-parameter optimization methodology through a simplified single-gain compensation strategy. Although Version-I demonstrated significant accuracy reductions in the rotor position error of RMS error of 43.04

rad to around 34.6 rad by optimization of five parameters its complexity and computational capabilities restricted its practical aspects of use in real time and ability to resist dynamic disturbances. To deal with these problems, version-II reformulates the optimization problem as just a single compensation gain (k), which intelligent scales the dead-time and harmonic effects, greatly reducing the computational load and making the convergence process much faster. Although the conditions that produce the distractions making the baseline RMS error as high as 1780.8 rad, the optimized Version-II nonetheless provides stability in estimation within a small error range (17801801 rad) and favors stability above aggressive error reduction. Particle Swarm Optimization and Simulated Annealing are metaheuristic algorithms with fast convergence times (4.39 s and 4.79 s, respectively), making them suitable to be used in real-time. In general, Version-II offers an effective, fast, and practically viable sensorless rotor position estimation system in SynRM drives to supplement the accuracy-oriented strategy in Version-I, and allows the framework to operate reliably in industrial settings with high demands.

References

[1] S. Yingjun, W. Zhenglong, and F. Yuanyuan, “An adaptive extended Kalman filter observer-for permanent magnet synchronous motor position sensorless control systems,” pp. 1–15, 2025.

[2] H. Cai and W. Luo, “Full-speed sensorless control system of synchronous reluctance motor with flux saturation model,” pp. 1–15, 2025.

[3] I. Ferdiansyah, “Dissertation Doctor of Engineering FPGA-based Sensorless Control Strategy for Permanent Magnet Synchronous Motor using High- Frequency Injection with Loaded Start-up Capability Graduate School of Life Science and Systems Engineering Department of Life Science and Systems Engineering Kyushu Institute of Technology Japan,” 2025.

[4] D. Studi, D. I. Parma, M. L. Tutor, A. S. Dottorando, and H. Sadeghlafmejani, “Self-Commissioning and Estimation Techniques for Sustainable Synchronous Reluctance Motor Drives in Industrial Applications,” 2025.

[5] Y. Ran, M. Qiao, L. Sun, and Y. Xia, “Review of Position Sensorless Control Technology for Permanent Magnet Synchronous Motors,” *Energies*, vol. 18, no. 9, 2025, doi: 10.3390/en18092302.

[6] S. Rigon, B. Haus, P. Mercorelli, and M. Zigliotto, “Comparison Between UKF and EKF in Sensorless Synchronous Reluctance Motor Drives,” *IEEE Open J. Power Electron.*, vol. 5, no. October, pp. 1562–1572, 2024, doi: 10.1109/OJPEL.2024.3469533.

[7] F. Zhang, S. Gao, W. Zhang, G. Li, and C. Zhang, “Current Sensor Fault-Tolerant Control Strategy for Speed-Sensorless Control of Induction Motors Based on Sequential Probability Ratio Test,” *Electron.*, vol. 13, no. 13, 2024, doi: 10.3390/electronics13132476.

[8] A. Xu, X. Li, S. Hu, and X. Liu, “Sensorless Control of Permanent Magnet-Assisted ermanent Magnet Assisted Synchronous Reluctance Motor,” vol. 117, no. October 2023,

pp. 33–40, 2024, doi: 10.2528/PIERL23103001.

[9] X. Liu, K. Liu, J. Li, and X. Zhao, "Sensorless Control of a Synchronous Reluctance Motor based on Improved Sliding Mode Control," vol. 10, no. 1, pp. 237–243, 2024, doi: 10.6919/ICJE.202401.

[10] G. Galati *et al.*, "Improved Sensorless Control of Multiphase Sensor Fault," vol. 5, no. 1, pp. 81–89, 2024.

[11] M. E. Boussouar, "Doctorat LMD en Electrotechnique Commande Sans Capteur de Vitesse du Moteur Synchrone à Reluctance Présentée par : Mohamed Essalih Boussouar Devant le jury composé de : Doctorat LMD en Electrotechnique Speed Sensorless Control of Synchronous Reluctance Motor Presented by : Board of Examiners :," 2024.

[12] W. Gayani and S. De Soysa, "New Sensorless Permanent Magnet Synchronous Motor Drive," no. August, 2024.

[13] P. Pramod and S. Member, "Position Sensing Errors in Synchronous Motor Drives," pp. 1–16, 2023.

[14] Z. Zhang and J. Lamb, "Active Q Flux Concept for Sensorless Control of," vol. 70, no. 5, pp. 4526–4536, 2023, doi: 10.1109/TIE.2022.3189090.

[15] S. Angayarkanni, K. Ramash Kumar, and A. Senthilnathan, "Comprehensive Overview of Modern Controllers for Synchronous Reluctance Motor," *J. Electr. Comput. Eng.*, vol. 2023, no. Iii, 2023, doi: 10.1155/2023/1345792.

[16] X. Jiang, C. Lin, J. Xing, Y. Xu, and Y. Tian, "A Global-Speed-Region Voltage Angle Control Method Considering Dead-Time Effect Compensation for Permanent Magnet Synchronous Motor Drives," *Actuators*, vol. 13, no. 12, 2024, doi: 10.3390/act13120530.

[17] M. Akrami, E. Jamshidpour, L. Baghli, and V. Frick, "Application of Low-Resolution Hall Position Sensor in Control and Position Estimation of PMSM—A Review," *Energies*, vol. 17, no. 17, pp. 1–20, 2024, doi: 10.3390/en17174216.

[18] P. Mercorelli, "Track Applications," 2023.

[19] Y. Huang, M. Zhao, Y. Wang, H. Zhang, and M. Lu, "An Improved Full-Speed Domain Sensorless Control Scheme for Permanent Magnet Synchronous Motor Based on Hybrid Position Observer and Disturbance Rejection Optimization," *Electron.*, vol. 12, no. 18, 2023, doi: 10.3390/electronics12183759.

[20] M. Murataliyev *et al.*, "Synchronous Reluctance Machines : A Comprehensive Review and Technology Comparison," 2022.